

Dissociative recombination angular distributions

Steven L. Guberman

Institute for Scientific Research, 22 Bonad Road, Winchester, MA 01890, USA

E-mail: slg@sci.org

Abstract. The angular distributions of the products of dissociative recombination of diatomic molecular ions are derived. The distributions are determined by the dominant partial waves of the captured electrons. For a single dominant wave, the neutral product distribution is described by the same spherical harmonic that describes the electron partial wave. The derived distributions take into account both direct and indirect dissociative recombination and are essential for modeling the projected distributions measured in storage ring experiments. All prior storage ring experiments have assumed that the product angular distributions can be described by spherical harmonics with angular momenta ≤ 1 and isotropic product distributions for "zero" eV electron capture. These assumptions are tested here by deriving the projected distributions for the dissociative recombination of CH^+ . For CH^+ , it is shown that the "zero" eV storage ring experimental results cannot be explained by only isotropic dissociation. Instead, an anisotropic model product distribution is required. The anisotropic model yields a quantum yield of 1.0 for $\text{C}({}^1D)$ instead of the incorrect value of 0.79 derived previously using an isotropic model. The quantum yields of all prior storage ring experiments on other molecular ions at "zero" eV electron energy must be reassessed in view of these findings.

1. Introduction

Many storage ring experiments have been reported in which the product quantum yields for dissociative recombination (DR) were measured (e.g. see Ref.'s [1]- [3]). The derivation of quantum yields from the storage ring data requires knowledge of the angular distribution of the products of DR. Until recently [4], there had been no published derivation of these distributions as a function of angle even though similar processes were treated in pioneering contributions many years ago. These include rules for dissociative attachment [5] and for electron impact excitation, capture and dissociative ionization for orientations of the internuclear axis both parallel and perpendicular to the electron beam [6]. A discussion of the nature of the angular distributions is especially important because in all the storage ring experiments reported to date, two questionable assumptions have been made: a) All quantum yields have been derived using electron partial waves having an angular momentum quantum number, $\ell \leq 1$ and b) The "zero energy" electron storage ring experiments have assumed that the electrons approach the ions isotropically, i.e. with no preferred direction. Both of these assumptions are examined below.

In Section 2, the angular distributions for the DR of diatomic molecules are described. Section 3 has a brief description of the storage ring method for determining quantum yields. Section 4 has an analysis of a prior experiment on CH^+ and shows how knowledge of the correct angular distributions (including waves with $\ell > 1$) is essential to a determination of accurate quantum yields. The conclusions are in Section 5.

2. Angular distributions

The coordinates are shown in Figure 1 where the electron with wave number \vec{k}_e is moving parallel to the laboratory fixed z axis and is at position \vec{r}_e with respect to the center of charge of the diatomic ion. The molecular axis lies at an angle θ from the positive z axis. The electron beam is taken to be cylindrically symmetrical about the z axis so that the angular distributions are independent of the angle φ (not shown in Figure 1) describing rotation of the internuclear axis around the z axis.

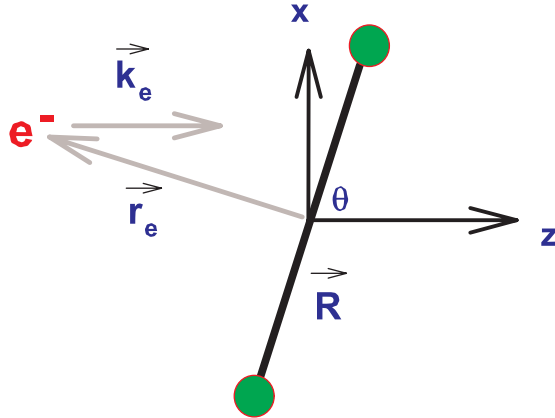


Figure 1. Coordinates for the approach of an electron, e^- , to a diatomic molecule lying at an angle θ from the positive z axis. See the text for the vector definitions.

2.1. Electronic Matrix Element

The source of the angular dependence is in the electronic coupling matrix element, V_{el} , which drives both capture and autoionization in DR:

$$V_{el}(\vec{k}_e, R) = \langle \psi_d(q, R) | H(q, R) | \psi_{vE}(q, \vec{k}_e, R) \rangle \quad (1)$$

where ψ_d is the electronic wave function of the dissociative state, H is the electronic Hamiltonian and ψ_{vE} is the initial wave function comprising the ion plus a continuum electron. q denotes the coordinates of all the electrons, v is the ion vibrational level and E is the total energy i.e. $E = k_e^2/2m + E_v$. Here E_v is the total energy of an ion vibrational level and m is the electron mass.

The initial wave function describing the ion plus a continuum electron in the ion coulomb field is given by:

$$\psi_{vE}(q, \vec{k}_e, R) = [\phi_{ion}(q^T, R) \phi_{\vec{k}_e}(\vec{r}_e)] \quad (2)$$

where q^T denotes the coordinates of the target or ion electrons. The right angle brackets indicate that the ion electrons and the continuum electron are antisymmetrized. The implicit dependence of the wave functions upon the internuclear distance is given by including R in parentheses.

The continuum electron can be expanded in Coulomb partial waves [7]:

$$\phi_{\vec{k}_e}(\vec{r}_e) = \sum_{\ell=0}^{\infty} (2\ell+1) i^\ell e^{i\sigma_\ell} \frac{1}{k_e r_e} F_\ell(k_e r_e) P_\ell(\hat{r}_e \cdot \hat{k}_e) \quad (3)$$

where F_ℓ is a confluent hypergeometric function, P_ℓ is a Legendre polynomial and σ_ℓ is the Coulomb partial wave phase shift. The expansion of the Legendre polynomial in spherical harmonics, $Y_{\ell m}$, where m is the projection of the electron partial wave angular momentum, ℓ , onto the internuclear axis, is given by [8]:

$$P_\ell(\hat{r}_e \cdot \hat{k}_e) = \frac{4\pi}{2\ell+1} \sum_{m=-\ell}^{\ell} Y_{\ell m}(\hat{r}_e) Y_{\ell m}^*(\hat{k}_e). \quad (4)$$

Substituting Equation (4) into Equation (3) gives:

$$\phi_{\vec{k}_e}(\vec{r}_e) = 4\pi \sum_{\ell=0}^{\infty} \sum_{m=-\ell}^{\ell} i^\ell e^{\sigma_\ell} \frac{1}{k_e r_e} F_\ell(k_e r_e) Y_{\ell m}(\hat{r}_e) Y_{\ell m}^*(\hat{k}_e). \quad (5)$$

Equation (1) can now be rewritten with the help of Equations (2) and (5):

$$V_{el}(\vec{k}_e, R) = 4\pi \left\langle \psi_d(q, R) | H(q, R) \left\{ \phi_{ion}(q^T, R) \sum_{\ell=0}^{\infty} \sum_{m=-\ell}^{\ell} i^\ell e^{\sigma_\ell} \frac{1}{k_e r_e} F_\ell(k_e r_e) Y_{\ell m}(\hat{r}_e) \right\} Y_{\ell m}^*(\hat{k}_e) \right\rangle. \quad (6)$$

Note that in Equation (6) both spherical harmonics have \vec{R} as the polar axis. Integrating over q , q^T , and r_e in Equation (6) leads to:

$$V_{el}(\vec{k}_e, R) = \sum_{\ell=0}^{\infty} \sum_{m=-\ell}^{\ell} V_{\ell m}(k_e, R) Y_{\ell m}^*(\hat{k}_e) \quad (7)$$

Equation (7) can be put into a more meaningful form by making use of a relationship between spherical harmonics due to O'Malley and Taylor [5]. $Y_{\ell m}^*(\hat{k}_e)$ in Equation (7) has \vec{R} as the polar axis with coordinates ϑ_R and ϕ_R . $Y_{\ell m}(\hat{R})$ has \hat{k}_e as the polar axis with coordinates ϑ_{k_e} and ϕ_{k_e} . In this case [5], $\vartheta_R = \vartheta_{k_e}$ and $\phi_R = -\phi_{k_e}$. From these considerations we have:

$$Y_{\ell m}^*(\hat{k}_e) = Y_{\ell m}^*(\vartheta_R, \phi_R) = Y_{\ell m}^*(\vartheta_{k_e}, -\phi_{k_e}) = Y_{\ell m}(\vartheta_{k_e}, \phi_{k_e}) = Y_{\ell m}(\hat{R}). \quad (8)$$

We can now rewrite Equation (7) as:

$$V_{el}(k_e, \vec{R}) = \sum_{\ell=0}^{\infty} \sum_{m=-\ell}^{\ell} V_{\ell m}(k_e, R) Y_{\ell m}(\hat{R}) \quad (9)$$

Equation (9) shows the angular dependence of the dissociating products, $Y_{\ell m}(\hat{R})$, for approach of electrons in the direction parallel to the z axis. Taking Λ_i and Λ_d to be the ion and dissociative state electron angular momentum projections on \hat{R} , respectively, the value of m is restricted by $\Lambda_d = \Lambda_i + m$. This restriction leads to a simplification of the summations in Equation (9). Once the electronic symmetries of the ion and dissociative states are specified, the value of m is fixed and Equation (9) can be rewritten as

$$V_{el}^m(k_e, \vec{R}) = \sum_{\ell=|m|}^{\infty} V_{\ell|m|}(k_e, R) Y_{\ell m}(\hat{R}). \quad (10)$$

In (10), the equivalence of $V_{\ell m}$ and $V_{\ell-m}$ have been used and accounted for by inserting a factor of 2 in $V_{\ell|m|}$. In some molecules, $V_{\ell|m|}$ is dominant and a single term describes the angular distribution,

$$V_{el}^m(k_e, \vec{R}) = V_{|m||m|}(k_e, R) Y_{|m|m}(\hat{R}). \quad (11)$$

At this point, the angular dependence of the electron capture matrix element has been demonstrated. The next Section uses this result to show how both direct and indirect DR are affected.

2.2. DR Angular Dependence

The complete derivation of the angle independent DR cross section expression can be found in earlier papers [9],[10]. In order to demonstrate the angular distributions, a slightly revised cross section is used here. We start with the expression for the total wave function:

$$\Psi(q, \vec{k}_e, R) = \sum_v \int dE' b_v(E') \psi_{vE'}(q, \vec{k}_e, R) \chi_v(R) + \psi_d(q, R) \zeta_d(R) + \sum_{p,v} a_{pv} \psi_p(q, R) \chi_v(R) \quad (12)$$

where the terms on the right from left to right describe the ion plus a Coulomb electron, the dissociative state and the Rydberg states. In (12), a_{pv} is the coefficient of vibrational level v in electronic Rydberg state p . Note that identical bound vibrational wave functions, $\chi_v(R)$, are used for both the ion and Rydberg states. $\zeta_d(R)$ is the dissociative state vibrational wave function. The final cross section expression from Ref. [10] can easily be generalized to multiple Rydberg levels:

$$\begin{aligned} \sigma_{DR}(\epsilon, \hat{R}) &= \frac{\pi^2 \omega \hbar K}{2\epsilon M} \left| \frac{1}{C} \left[-V_{v_i}(E, \hat{R}) + i\pi \sum_v d_v V_v(E, \hat{R}) - \sum_{pv} V_v(E, \hat{R}) \rho_p a_{pv} \right. \right. \\ &\quad \left. \left. + i\pi \sum_{pv} \sum_{v'} V_{v'}(E, \hat{R}) \rho_p a_{pv} W_{vv'} \right] \right|^2 \end{aligned} \quad (13)$$

where C is a Wronskian (see [10]) and $\rho_{n^*} = (n^*)^{-3/2}$ where n^* is the effective principal quantum number. In (13), ϵ is the electron energy, ω is the statistical weight of the dissociative state divided by that for the ion, K is the relative momentum of the dissociating atoms, M is the total reduced mass, $W_{vv'}$ is the vibronic coupling between the ion level and the Rydberg levels, i.e. $W_{vv'} = (v'/2M\omega_e)^{1/2} d\mu/dR$. Here $v' = v + 1$, ω_e is the vibrational frequency of the ion and μ is the quantum defect of the Rydberg series. d_v is given by

$$d_v = \langle \chi_v(R) | V_{\ell|m|}(k_e, R) | \zeta_d(R) \rangle. \quad (14)$$

In (13), the matrix elements V_{v_i} and V_v are given by

$$\begin{aligned} V_{v_i}(E, \hat{R}) &= \int \chi_{v_i} V_{el}^m(k_e, \vec{R}) F_{1E}(R) dR \\ V_v(E, \hat{R}) &= \int \chi_v V_{el}^m(k_e, \vec{R}) F_{1E}(R) dR \end{aligned} \quad (15)$$

where the v_i subscript denotes the initial ion vibrational level and $F_{1E}(R)$ is a solution of:

$$\left(\frac{-\hbar^2}{2M} \frac{d^2}{dR^2} + E_d(R) - E \right) F_{1E}(R) = 0. \quad (16)$$

If electron capture is dominated by a single partial wave, Equation (11) may be used in Equations (15) to give

$$\begin{aligned} V_{v_i}(E, \hat{R}) &= Y_{\ell m}(\hat{R}) \int \chi_{v_i} V_{\ell|m|}(k_e, R) F_{1E}(R) dR \\ V_v(E, \hat{R}) &= Y_{\ell m}(\hat{R}) \int \chi_v V_{\ell|m|}(k_e, R) F_{1E}(R) dR \end{aligned} \quad (17)$$

For a single dominant partial wave, the cross section can be written as:

$$\begin{aligned} \sigma_{DR}(\epsilon, \hat{R}) &= \frac{\pi^2 \omega \hbar K}{2\epsilon M} \left| Y_{\ell m}(\hat{R}) \right|^2 \left| \frac{1}{C} \left[-V_{v_i}(E) + i\pi \sum_v d_v V_v(E) - \sum_{pv} V_v(E) \rho_p a_{pv} \right. \right. \\ &\quad \left. \left. + i\pi \sum_{pv} \sum_{v'} V_{v'}(E) \rho_p a_{pv} W_{vv'} \right] \right|^2. \end{aligned} \quad (18)$$

where

$$\begin{aligned} V_{v_i}(E) &= \int \chi_{v_i} V_{\ell|m|}(k_e, R) F_{1E}(R) dR \\ V_v(E) &= \int \chi_v V_{\ell|m|}(k_e, R) F_{1E}(R) dR. \end{aligned} \quad (19)$$

From Equation (18), for a single dominant electron partial wave, the angular dependence of the DR cross section is given by $|Y_{\ell m}(\hat{R})|^2$. Therefore, the neutral DR products have the same angular dependence as the partial wave of the incoming Coulomb like electron. The angular distributions are spherical harmonics and are listed with appropriate normalization constants in Table I of Reference [4]. For each possible electron partial wave up to $\ell = 3$, Tables II and III of Reference [4] have all possible product electronic symmetries formed by capture by a diatomic ion in several electronic symmetries.

In these calculations, the slow rotation approximation has been used. It is assumed that the molecular axis does not change its orientation in the brief time between electron capture and molecular dissociation.

It is important to recognize that for a single dominant partial wave, the angular dependence for the dissociation products is similar to that found for dissociative attachment (DA) [5] even with the inclusion of indirect recombination through intermediate Rydberg states of the same symmetry. Note that the dissociative attachment analogue of indirect DR was not treated previously [5]. If more than one partial wave is important, the angular distribution is given by Equation (13).

3. Storage Ring Quantum Yield Measurements

A sketch of a section of a storage ring containing the electron cooler is shown in Figure 2. In the electron cooler, an electron beam is merged with and velocity matched to a colinear ion beam. Collisions between the electrons and ions reduce the momentum spread of the ion beam causing it to contract to a diameter that is considerably less than that of the electron beam. The contraction allows for the injection of more ions into the ring leading to a bright ion beam and a high signal for the neutral products of DR. The electron beam is removed from the ion beam by a magnet and is continuously renewed. In addition to cooling, DR and other processes occur in the electron cooler. The center of mass of the resulting neutral DR products continues at approximately the ion beam speed to a multichannel plate where an electron avalanche is generated by the impinging neutral particles. This avalanche causes a spot to glow on a phosphor

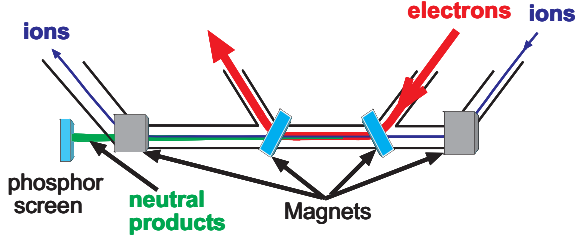


Figure 2. A section of a storage ring showing the electron cooler where ion and electron beams merge. The neutral DR products generated in the cooler are detected by a phosphor screen.

screen. The distance between the two spots due to a single DR event is recorded electronically. Measurements of many DR events generate a distribution of distances for a single electron energy. The recorded distance between the impinging particles is determined by the ion beam velocity, the distance from the point of recombination to the multichannel plate, the DR kinetic energy release and the angular distribution of the products. The distance spectra are fit to model projected distributions. From the fit, the quantum yields can be determined. This ingenious technique was first described in pioneering measurements on HD^+ [11]. An excellent detailed description of the quantum yield measurements can also be found in the pioneering paper on CH^+ [1].

The reliability of the deduced quantum yields is dependent upon an accurate knowledge of the product angular distributions. If several product asymptotes (i.e. kinetic energy releases) are energetically allowed, the angular distribution of each channel must be included. The prior section shows that the angular distributions are given by spherical harmonics. However, to date, the recorded distance spectra for all reported storage ring quantum yield measurements have been fitted with model distributions that include only isotropic, $\sin^2\theta$ and $\cos^2\theta$ angular distributions. In addition, the "zero eV" measurements have all assumed that only isotropic distributions are needed. These assumptions are tested in the next section.

4. Quantum Yields for CH^+

Here, I discuss the pioneering storage ring measurements on CH^+ [1] in the context of the angular distributions described above. The ground state of CH^+ has ${}^1\Sigma^+$ symmetry and the main DR route has long been known [12]-[14] to be ${}^2\Pi$ which dissociates to $\text{C}({}^1D) + \text{H}$ where H is in its ground state. The electronic symmetries of these states require that the captured electron have π symmetry. Tables I and III in Reference [4] show that the expected product angular distributions are $(3/2)\sin^2\theta$ for $\ell = 1$ ($p\pi$), $(15/2)\sin^2\theta\cos^2\theta$ for $\ell = 2$ ($d\pi$) and $(21/16)\sin^2\theta(5\cos^2\theta - 1)^2$ for $\ell = 3$ ($f\pi$) where θ is the angle between the internuclear axis and the laboratory z axis of Figure 1. The $\ell = 3$ capture width is expected to be small and this partial wave is not treated here. Model projected distributions are shown in Figure 3. The isotropic and $\sin^2\theta$ model distributions have been calculated previously [1],[15].

The experimentally measured distribution is shown by the histogram plot in Figure 4 which is from Figure 11(b) of Reference [1]. For these results, the electrons are velocity matched with the ions and have a relative energy of "zero" eV. However, the electrons have a flattened energy distribution with $kT_{\perp} = 17\text{meV}$ and $kT_{\parallel} = 0.5\text{meV}$. At zero energy, it was assumed [1] that the electrons approach the ions isotropically. One can show that for isotropic approach, an isotropic distribution of products is generated even if the electron is captured into an orbital with $\ell \neq 0$. Although the electron energy distribution is anisotropic, the experimentalists assume that at "zero" eV, the electron capture is isotropic and the product distribution is isotropic. With this assumption, they fit the measured distribution to model isotropic distributions arising from all

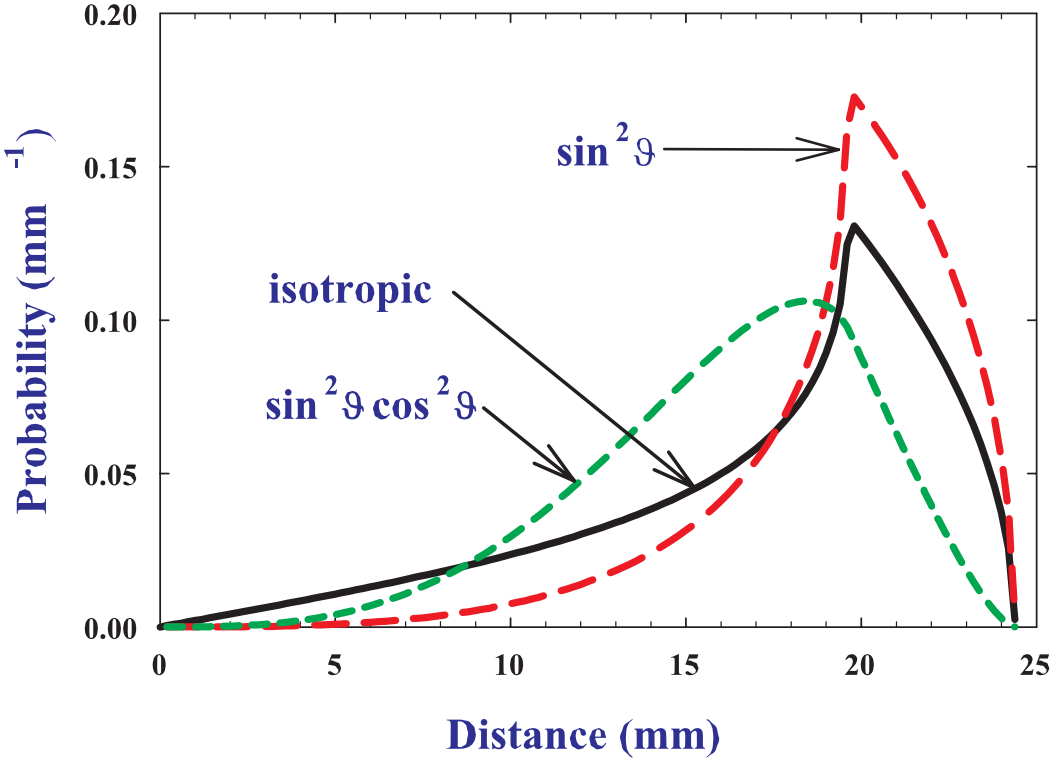


Figure 3. Model projected distributions for CH^+ for DR along the $2^2\Pi$ route. The model distributions are appropriate for the experimental setup of Reference [1].

the accessible atomic asymptotes. Following this, they allow $\sin^2\theta$ and $\cos^2\theta$ distributions to mix in with adjustable coefficients. They find that the anisotropic contributions are less than the $\pm 10\%$ error bars. The resulting fit gives a $79\% \pm 10\%$ branching to $\text{C}(^1D) + \text{H}(^2S)$ and a $21\% \pm 10\%$ branching to $\text{C}(^1S) + \text{H}(^2S)$. The isotropic model fit to the experimental data is excellent (see the short dashed line in Figure (4)).

Dissociation to $\text{C}(^1S) + \text{H}(^2S)$ must utilize the potential curve for $2^2\Sigma^+$, the only state leading to this asymptote. However, this state does not cross the ion [16] but crosses the dissociative, $2^2\Pi$ state near 3.2 Bohr. The authors suggested that dissociation could begin on the main DR route, $2^2\Pi$, and then transfer to the $2^2\Sigma^+$ state at the crossing by a rotational or spin-orbit coupling. The rotational coupling and potential curves of Reference [16] were used [17] in Landau-Zener and close coupling calculations for these two states. It was found [17] that the rotational coupling is too small to account for a transition between these states during dissociation. Separate calculations [18] of the spin-orbit matrix element indicate that it is also too small to significantly couple these states. It has also been suggested [17] that it may be possible to dissociate along the $2^2\Sigma^+$ state if it can capture the incoming electron via a Born-Oppenheimer breakdown coupling mechanism as has been shown to occur in HeH^+ DR [19]. However, the prior calculations [16] and calculations completed in this laboratory [18] show that at the energy of the ion $v=0$ level, the $2^2\Sigma^+$ state is much further from the ion $v=0$ inner turning point than is the case for the most important dissociative state in HeH^+ DR. Therefore, this mechanism is predicted to be unimportant for CH^+ DR.

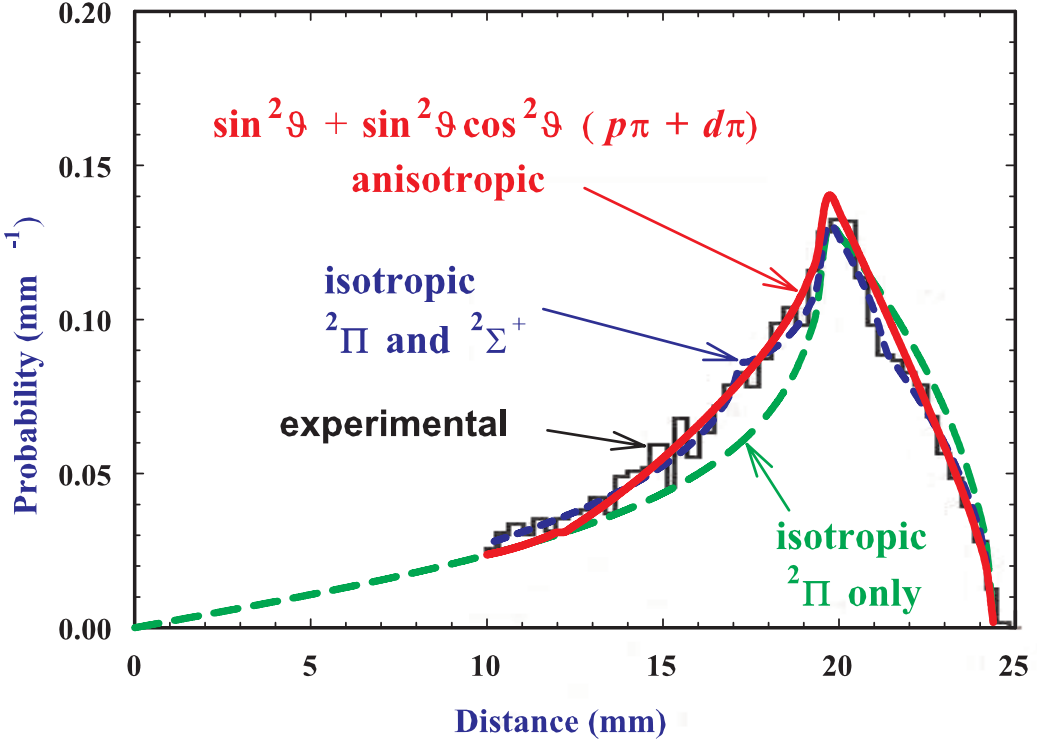


Figure 4. Experimental projected distribution (thin solid line) from Figure 11b of Reference [1]. Also shown are the model projections for isotropic dissociation along $2^2\Pi$ and $2^2\Sigma^+$ (short dashed line, blue in online version), isotropic dissociation along $2^2\Pi$ only (long dashed line, green in online version) and anisotropic dissociation along $2^2\Pi$ using $\ell = 1, 2$ partial waves(thick solid line, red in online version).

Since the $2^2\Sigma^+$ state cannot participate in DR, dissociation must take place exclusively along $2^2\Pi$. The model projected distribution along $2^2\Pi$ for isotropic electron capture is shown by the long dashed line in Figure 4. This model projection does not fit the experimental data in the region of 14-19 mm. The results indicate that at “zero” eV, capture by an entirely isotropic mechanism does not reproduce the experimental results.

A calculation [14] of the DR cross section for CH^+ has shown that the $\ell = 1$ ($2p\pi$) and $\ell = 2$ ($3d\pi$) electron partial waves have nearly equal electron capture widths. Using this information, the model projected distributions have been calculated for dissociation along only $2^2\Pi$ with a superposition of equal parts of ($2p\pi$) and ($3d\pi$) partial wave capture. The results are shown by the solid line (red in online edition) in Figure 4. This approach reproduces the experimental data quite well except for a small deviation at 21-22 mm. Note that between 10-12 mm, a small overlapping contribution from the DR of $a^3\Pi$ ions has been added to the model fit. Clearly, the experimental data can be represented quite well with model projections that describe an anisotropic approach of the electrons to the ions. Further details of these calculations will be published separately [18].

5. Conclusions

The angular product distributions generated from the DR of diatomic molecular ions have been reviewed. Both direct and indirect DR are included in the approach. The magnitudes of the electron partial wave capture widths determine which partial waves dominate DR. The dominant partial waves directly determine the product angular distributions. For the case of a single dominant partial wave, the spherical harmonic describing the product distribution is identical to that for the electron partial wave in the slow rotation approximation. The angular distributions are identical to those derived previously for dissociative attachment (DA) [5] even though the analogue of indirect DR was not included in the treatment of DA.

The small couplings found for the $2^2\Sigma^+$ state eliminate the possibility of generating C(1S) from DR of CH $^+$. Therefore, the quantum yield for C(1D) is 1 and not 0.79 as originally suggested from the fitting of isotropic only distributions[1].

The experimental projected distribution at "zero" eV is described quite well by an anisotropic distribution having $\ell = 1$ and 2 contributions and cannot be described solely by an isotropic distribution. These results indicate that the electrons approaching the ions in the experiment do not approach in an entirely isotropic manner as has been assumed in the interpretation of the data from all "zero" eV storage ring experiments, not just the experiment described here on CH $^+$. The quantum yields derived from storage ring experiments at "zero" eV must all be reassessed.

Acknowledgments

This paper is based upon work supported by the National Science Foundation under Grant No. ATM-0225256. This research was also supported by NASA Grants NAG5-12220, NAG5-11827 and NAG5-11428.

References

- [1] Amitay Z, Zajfman D, Forck P, Hechtfischer, Seidel B, Grieser M, Habs D, Repnow R, Schwalm D and Wolf A 1996 *Phys. Rev. A* **54** 4032
- [2] Peterson J R et al. 1998 *J. Chem. Phys.* **108** 1978
- [3] Vejby-Christensen L, Kella D, Pedersen H B, Andersen L H 1998 *Phys. Rev. A* **57** 3627
- [4] Guberman S L 2004 *J. Chem. Phys.* **120** 9509
- [5] O'Malley T F and Taylor H S 1968 *Phys. Rev.* **176** 207
- [6] Dunn G 1962 *Phys. Rev. Lett.* **8** 62
- [7] Bransden B H 1970 *Atomic Collision Theory* (New York: Benjamin) p. 104
- [8] Mathews J and Walker R L 1970 *Mathematical Methods of Physics* (Menlo Park: Benjamin/Cummings)
- [9] Bardsley J N 1968 *J. Phys. B* **1** 365
- [10] Giusti-Suzor A, Bardsley J N and Derkits C 1983 *Phys. Rev. A* **28** 682
- [11] Zajfman D, Amitay Z, Broude C, Forck P, Seidel B, Grieser M, Habs D, Schwalm D and Wolf A 1995 *Phys. Rev. Lett.* **75** 814
- [12] Bardsley J N and Junker B R 1973 *Ap. J.* **183** L135
- [13] Krauss M and Julienne P S 1973 *Ap. J.* **183** L139
- [14] Takagi H, Kosugi N and Le Dourneuf M 1991 *J. Phys. B* **24** 711
- [15] Kella D, Johnson P J, Pedersen H B, Vejby-Christensen L and Andersen L H 1996 *Phys. Rev. Lett.* **77** 2432
- [16] van Dishoeck E 1986 *J. Chem. Phys.* **86** 196
- [17] Carata L, Orel A E, Raoult M, Schneider I F and Suzor-Weiner A 2000 *Phys. Rev. A* **62** 052711
- [18] Guberman S L, to be published.
- [19] Guberman S L 1994 *Phys. Rev. A* **49** R4277